Nonlinearity **10** (1997) 1599–1614. Printed in the UK PII: S0951-7715(97)79427-1

Mathematical modelling of capsule formation and multinodularity in benign tumour growth

Abbey J Perumpanani†‡‖, Jonathan A Sherratt†§ and John Norbury‡

† Mathematics Institute, University of Warwick, Coventry CV4 7AL, UK
‡ Mathematical Institute, 24-29 St Giles', Oxford OX1 3LB, UK
§ Department of Mathematics, Heriot-Watt University, Edinburgh EH14 4AS, UK

Received 11 November 1996, in final form 14 July 1997
Recommended by H Levine

Abstract. Tumours that grow locally, but do not invade the surrounding tissue are called benign. Such benign tumours are characterized by the presence of a surrounding band of connective tissue called a capsule. In some cases, the tumours are also broken into a number of discrete nodules. In this paper the authors use a partial differential equation model to study the interactions of a growing tumour with the surrounding tissue. They predict mechanisms for both capsule formation and nodularity. The former has the mathematical form of bifurcation from travelling waves to aggregating waves of connective tissue, resulting in the accretion of connective tissue in a manner corresponding to capsule formation. The cause of multilobularity in tumours is currently not known. Using their model, the authors are able to predict lobulation, when tumour cell motility is retarded by aggregating connective tissue. In the final part of the paper, the authors introduce an enlarged model, and use it to demonstrate both capsule formation and the possible dissolution of the capsule following a mutation resulting in the production of proteases by the cancer cells.

AMS classification scheme numbers: 92, 35

1. Introduction

The presence of a capsule around a tumour is the most significant gross morphological feature determining the clinical outcome. Tumours that are encapsulated (that is, having a dense band of surrounding connective tissue) have a favourable prognosis and only produce symptoms related to pressure effects on surrounding tissue [3]. Such tumours are known as benign. Malignant tumours, on the other hand, do not have a well circumscribed capsule; the cancerous cells invade neighbouring tissue and are carried far from their primary site by the metastatic cascade [2]. Malignant tumours are potentially lethal and may either arise *de novo* or in existing benign tumours which may be encapsulated. In the latter case the cancerous cells have to disrupt the capsular barrier before spreading further.

Any normal tissue in the body may be viewed simplistically as a collection of different types of cells anchored into position by the presence of intervening extracellular matrix. Among other elements, this extracellular matrix is composed of strands of connective tissue fibres such as collagen, elastin, fibronectin, etc [25]. A tumour arises when one of the cells (or sometimes a few) proliferates more rapidly than its neighbours. This aggressive

‖ E-mail address: abbey@maths.warwick.ac.uk

0951-7715/97/061599+16$19.50

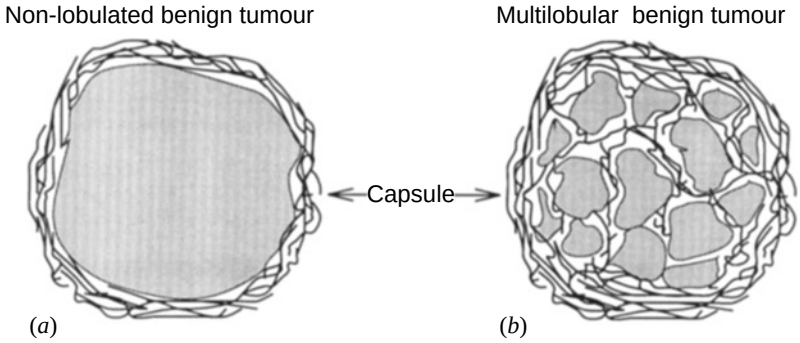

Figure 1. Schematic representation of two morphological variants of benign tumours. (*a*) The gross appearance of an encapsulated but non-lobulated tumour. Typical tumour capsules range from 0.13 to 3.09 mm in cross section (mean ± standard deviation = 0.87 ± 0.59 mm) [18]. (*b*) A multilobulated tumour in which the different lobules are separated by intervening strands of connective tissue. The cause of lobulation in tumours is not known; in section 5 we describe a mechanism by which such lobulation can arise. A typical tumour capsule shows wide variability in its thickness. In a clinico-pathologic study on patients with hepatocellular carcinomas, Ng *et al* [18] reported that the tumour capsule ranged from 0.13 to 3.09 mm (mean ± standard deviation = 0.87 ± 0.59 mm).

proliferation may be the result of a mutation which encourages division, or one that makes the cell deaf to the inhibitory growth signals from its neighbours [20]. In any case the result is a group of cells proliferatively outpacing the neighbouring cells and producing a localized growth—a benign tumour. The pathological hallmark of such a benign tumour is the presence of a dense band of connective tissue around it—the capsule. The capsule is composed chiefly of matrix fibres; we use the term 'connective tissue' throughout, following convention. In this paper we begin by considering the mechanism of capsule formation, using a mathematical formulation of existing ideas on encapsulation. We will use a combination of analytical and numerical techniques to describe the mathematical analogue of encapsulation as a bifurcation from a constant shape wave to an aggregating wave of connective tissue.

An unsolved problem in tumour biology is the cause of multinodularity in some benign tumours. Benign tumours may either be a single mass with a surrounding capsule (non-lobulated), or may be broken into nodules of varying size with additional intervening strands of connective tissue (multilobulated); this is schematically shown in figure 1. In the second part of the paper, we use the model to study the effect of a progressively thickening capsule retarding the movement of the tumour cells and show that this provides a simple explanation for the transformation of a simple non-lobulated tumour into a multilobulated form. We also suggest an experimental approach to testing our explanation.

Many tumour cells secrete enzymes that degrade components of extracellular matrix. For example, squamous cell carcinomas, particularly from the cervical lymph nodes, can digest the capsular collagen through proteases synthesized by the tumour and tumour-associated stroma [8]. In the final part of the paper, we use an enlarged model to demonstrate the transcapsular spread of cancer cells caused by a mutation resulting in the production of a protease in the cells of a pre-existing benign tumour. The clinical implications of such a transcapsular spread have long been recognized and it is now regarded as an important prognostic factor, in particular for local recurrence of tumours in the neck [28].

2. Theories of capsule formation

Traditionally, there have been two schools of thought about the formation of a tumour capsule. According to the *expansive growth hypothesis*, a benign tumour becomes surrounded by a capsule when the adjoining connective tissue is passively convected by the expanding tumour and the cellular elements undergo pressure atrophy; the extracellular collagenous matrix becomes condensed into a circumferential capsule. Berenblum [6] observed that tumours growing within the lumen of a hollow organ, or on the surface of the body, do not become encapsulated, a finding that Berenblum suggests confirms the hypothesis that capsules can only be formed in situations where a tumour can exert pressure on surrounding tissue. According to the expansive growth hypothesis, the appearance of a fibrous capsule is essentially a passive phenomenon, and the capsular collagen is derived from mature pre-existing collagen rather than being newly deposited. The aggregation of connective tissue represents the cumulative effect of a series of lower level interactions at the interface of the expanding tumour and the convected connective tissue.

Another school of thought about the mechanism of capsule formation is the *foreign-body hypothesis*. This view is essentially of an active process where the body mounts a response akin to inflammation to create a fibrous barrier. Ewing [10] wrote of the 'controlling influence of encapsulation', suggesting that the encapsulated tumours may 'thus be shielded from cellular attack'. Similarly, Enneking [9] wrote of the hosts attempt to 'encapsulate and contain tumours'. However, evidence from various sources suggests that the foreign-body hypothesis is unlikely. For instance, none of the human tumours in which tumour-specific or tumour-associated antigens have been identified are associated with an encapsulated growth edge [4]. Hence, at best the foreign-body hypothesis has limited application. Barr *et al* [5] gave a detailed review of the mechanisms of encapsulation and also suggested a compromise hypothesis embodying both of the above mechanisms.

3. Formulation of the model

We derive a model for the growth of a benign tumour based on a continuum approach, in which $m(x,t)$ and $c(x,t)$ represent the concentrations of the tumour cells and connective tissue respectively. Here x and t are the space and time coordinates. The model studies the averaged behaviour of the tumour cells in the direction of expansion only, and ignores variations in the plane perpendicular to the direction of growth.

In the absence of any surrounding connective tissue we describe the local proliferation of the benign tumour cells by $f(m)$ and the flux of the cells by J_m, say. However, the presence of connective tissue will influence the movement of the benign tumour cells. We describe the effects of connective tissue on the motility of tumour cells by $\theta(c)$, and model the overall flux of the tumour cells by the product $\theta(c)J_m$. Based on the expansive growth hypothesis stated earlier, we model the connective tissue flux as being proportional to the flux of the cells, that is, $\theta(c)J_m$. This is the appropriate flux term since the density of connective tissue c is measured per unit volume rather than per cell. In practice, there should be a separate saturation term, in addition to $\theta(c)$, representing the limitation on matrix reorganization potential per cell. However, since we already have a saturation effect via $\theta(c)$, we omit this term for simplicity. Under these assumptions we write the model for benign tumour growth as

$$\frac{\partial m}{\partial t} = f(m) + \frac{\partial}{\partial x}[\theta(c)J_m] \tag{1a}$$

$$\frac{\partial c}{\partial t} = k\frac{\partial}{\partial x}[c\theta(c)J_m]. \tag{1b}$$

Our approach is based on the prediction of Sherratt and Nowak [21] that the early growth of a tumour has the form of a travelling wave moving outwards from an initial site of disease into the surrounding normal tissue. The increase in tumour size is primarily driven by cell division; cell movement is just local random motion at the tumour edge. We use simple functional forms of f and J_m which give travelling wave solutions reminiscent of those demonstrated by Sherratt and Nowak [21]. The advantage of such a generic model approach is that the ensuing simplicity allows an analytical appraisal of the equations while retaining the necessary qualitative features. Throughout, we describe the proliferation of tumour cells using the logistic growth model which Vaidya and Alexandro [24] established as an appropriate model for tumour cell growth. Under an appropriate rescaling of tumour cell density m and time t, this gives $f(m) = m(1-m)$.

We assume that the boundary does not have any significant bearing on the evolution of the tumour and hence study the case of an infinite domain, which in our numerical simulations is represented by a large finite domain with zero derivative conditions on the boundary. We assume that at time $t = 0$, the tumour cell population is zero except in a small region centred at $x = 0$. We take the initial connective tissue density $c(x, 0)$ to be zero near this region, and a non-zero constant (set arbitrarily to 0.2) away from it. The results of the simulations are not sensitive to the details of these initial conditions. To reduce the simulation time, we solve only on the region $x \geqslant 0$, using a symmetry boundary condition at $x = 0$.

4. Connective tissue waves and capsule formation

We begin by considering model (1) in the simple case of $\theta(c) \equiv 1$, that is, changes in connective tissue density have no effect on cell motility. This case will be relevant during the early stages of tumour growth, in which connective tissue accretion on the surface of the tumour is too low to significantly restrain its expansion. Moreover, study of this simple case gives important mathematical insights into the behaviour of more general forms of $\theta(c)$.

We have solved equations (1) numerically with $\theta(c) \equiv 1$ for two different forms for the cell flux. The first case is $J_m = \partial m/\partial x$, in which case (1*a*) becomes the very well studied Fisher equation [17]. Standard theory [14] shows that for this equation, initial conditions of the form we are using for m evolve to a travelling wave, moving with constant shape and with speed 2. Secondly, we have considered $J_m = m\partial m/\partial x$, giving the nonlinear Fisher equation, for which our initial conditions evolve to a sharp-front travelling wave, moving with speed $1/\sqrt{2}$ [16, 22]. Our interest is in the way in which connective tissue is convected by these waves of cell density.

Numerical simulations show that for both flux terms, the solution for c depends critically on the parameter k, which reflects the strength of connective tissue convection. When k is small, a wave of connective tissue moves in parallel with the wave of tumour cells, with the effect that a constant band of connective tissue is pushed ahead by the growing tumour (figure 2). However, when k increases above a critical value, the form of the solution alters significantly, and the peak in the c-wave increases with time, corresponding to a gradually increasing intensity of the predicted capsule (figure 3).

Before launching into a detailed mathematical analysis of these results, we present a simple intuitive explanation for the change in behaviour. In equation (1*b*) with $\theta(c) \equiv 1$, kJ_m is the velocity at which connective tissue is being convected, while a is the speed of the

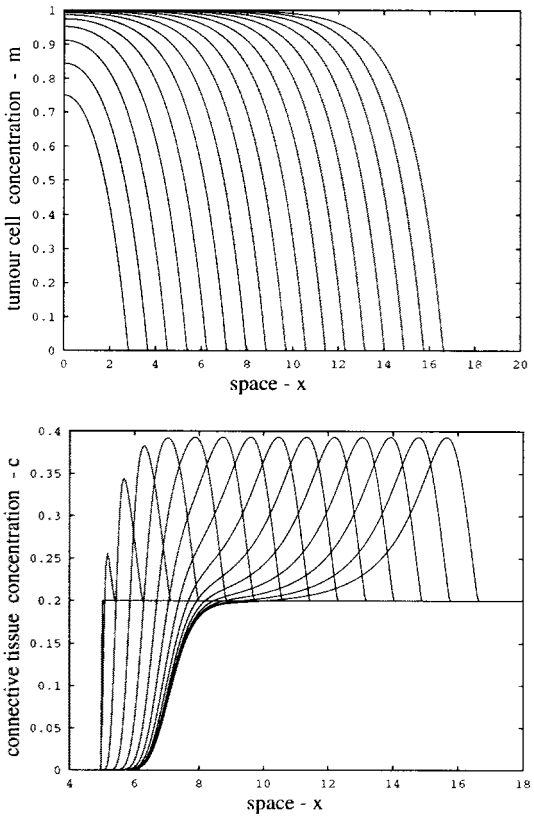

Figure 2. Numerical solutions of equations (1) with $k = 3.8$, $\theta(c) \equiv 1$, and $J_m = m\partial m/\partial x$. In this case the bifurcation value of k is 4. We plot m and c as functions of space at equal intervals of time. Both the m and c waves eventually evolve into constant shape travelling waves.

tumour cell wave. When the velocity of the connective tissue wave is slower than that of the cell wave, we expect only a fleeting ripple to be produced in the solution for c. However, when $kJ_m > a$ at some points, the ECM at these points is actually convected faster than the speed at which the cell wave moves, causing a build up of connective tissue. An analogous physical situation is the difference between the rippling of the surface of a cornfield by wind (small k) and a gust of wind blowing loose strands of hay into a pile (large k). In the following analysis, we will show that the bifurcation value of k, at which the c-wave changes from a constant shape wave to an aggregating wave, is indeed $k = a/\max\{J_m\}$.

We will study this case of $\theta(c) \equiv 1$ analytically, with two key objectives: to determine the value of k at which the c-wave changes form, and the rate at which the peak of c increases when k is above this value. We denote by $M(z)$ the sharp front travelling wave solution of $(1a)$ that evolves from our initial conditions; here $z = x - at$ where a is the speed of this cell wave. In the case of the nonlinear Fisher equation, a closed form expression for $M(z)$ exists, but not for the Fisher equation. In either case, J_m depends only on M and its derivatives, and can thus be written as a function of z, say $J(z)$.

Rewriting $(1b)$ in terms of coordinates $\tau = t$ and $z = x - at$ gives

$$\frac{\partial c}{\partial \tau} + [kJ(z) - a]\frac{\partial c}{\partial z} = -kJ'(z)c. \tag{2}$$

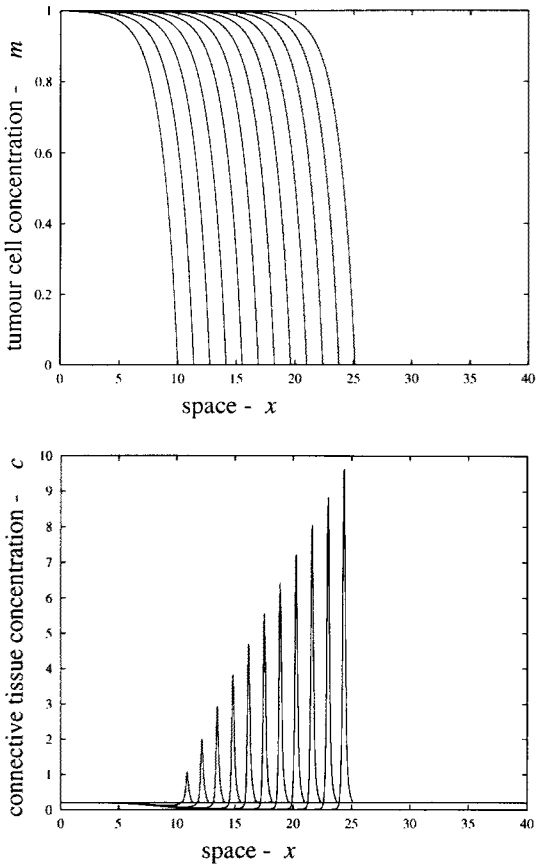

Figure 3. Numerical solutions of equations (1) with $k = 4.05$, $\theta(c) \equiv 1$, and $J_m = m\partial m/\partial x$. In this case the bifurcation value of k is 4. We plot m and c as functions of space at equal intervals of time measuring 1.9. The solution has the form of a constant shape travelling wave for m and an aggregating wave for c. We used $c(0) \equiv 0.2$ as the initial condition for c to best illustrate the mathematical properties of the solution, as described in the main text. In the case of a step function form of $c_0(.)$, which is the initial condition used in figure 2, this multiplication by $c_0(\theta)$ would have the effect of removing the trough in the solution for $c(z, \tau)$, although the growing peak remains.

This first-order partial differential equation can be solved exactly using the method of characteristics, and we will use this method to determine the qualitative form of the solution for $c(z, \tau)$ for general $J(\cdot)$. Of course, in practice the solution for $m(x, t)$ only approaches $M(z)$ asymptotically as $t \to \infty$, and thus our solution for c will also only be exact in this limit.

The qualitative form of $J(z)$ is illustrated in figure 4, and is the same for any realistic flux expression. Crucially, we will assume that $J(z) \geqslant 0$ for all z, with $J(z) \to 0$ as $z \to \pm\infty$, and $J'(z)$ non-zero except at the unique local maximum, at which $J(z) = J_{\max}$, say. In the case of nonlinear cellular diffusion, $J(z)$ is identically zero for sufficiently large z, since the m-wave is of sharp-front type, but this will not be significant in our calculations.

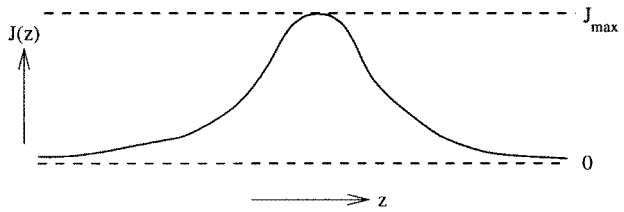

Figure 4. The qualitative form of the cell flux $J_m = J(z)$ when cell movement is not hindered by extracellular matrix levels.

The characteristics of (2) are given by solving

$$\mathrm{d}\tau = \frac{\mathrm{d}z}{kJ(z) - a} = \frac{-\mathrm{d}c}{kJ'(z)c}$$

which gives the two characteristic functions

$$\mathcal{C}_1(c, z) = c/c_{tw}(z) \qquad \text{and} \qquad \mathcal{C}_2(\tau, z) = \tau - G(z)$$

where

$$c_{tw}(z) = 1/[a - kJ(z)] \qquad \text{and} \qquad G(z) = -\int c_{tw}(z)\,\mathrm{d}z.$$

Thus, the solution for c is given by eliminating the parameter θ, say, from

$$\frac{c}{c_{tw}(z)} = \frac{c_0(\theta)}{c_{tw}(\theta)} \qquad \text{and} \qquad G(z) - \tau = G(\theta). \tag{3}$$

Here $c_0(x) \equiv c(x, t = 0)$. The key determinant of the form of this solution is the sign of $kJ_{\max} - a$. If this expression is negative, then $\mathcal{C}_1(c, z)$ is finite for all z, so that a possible solution is $c(z, \tau) = c_{tw}(z)$, independent of τ. This is a travelling wave solution for c, and it is straightforward to show, using the method of characteristics, that all bounded initial conditions evolve to this solution, multiplied by $c_0(\theta)$, as $\tau \to \infty$.

The case $kJ_{\max} > a$ is more complicated, however (figure 5). Then $c_{tw}(z)$ has the qualitative form illustrated in figure 5(*b*), with infinities at the points, z_1 and z_2 say ($z_1 < z_2$), at which $kJ(z) = a$. Thus, the solution for c cannot be of travelling wave form, and must be determined from (3). Integrating c_{tw} shows that $G(z)$ has the qualitative form illustrated in figure 5(*c*), also with infinities at z_1 and z_2. In order to use solution (3), we require the parameter θ, which is given by $\theta(z, \tau) = G^{-1}[G(z) - \tau]$; here G^{-1} denotes the local inverse. The qualitative form of θ as a function of z at successively increasing τ is illustrated in figure 5(*d*). Crucially $\theta(z_1, \tau) \equiv z_1$ and $\theta(z_2, \tau) \equiv z_2$.

For simplicity, we begin by considering the case $c_0(x) \equiv 1$, so that (3) implies $c(z, \tau) = c_{tw}(z)/c_{tw}(\theta(z, \tau))$. The qualitative form of $c_{tw}(\theta)$ as a function of z at increasing τ is illustrated in figure 4(*e*), and compared with $c_{tw}(z)$. However, from these sketches alone it is not possible to determine the form of the ratio $c_{tw}(z)/c_{tw}(\theta)$, since the behaviour near $z = z_1$ and $z = z_2$ is not clear, and requires detailed analysis.

For z close to z_1, $kJ(z) - a \approx \lambda(z - z_1)$, where $\lambda = kJ'(z_1)$; our assumption that $J'(z) \neq 0$, except at the unique maximum, implies that $\lambda > 0$. Thus, to leading order near $z = z_1$,

$$G(z) = \lambda^{-1} \log|z - z_1|$$
$$\Rightarrow G^{-1}(\xi) = z_1 + \exp(\lambda\xi)\mathrm{sign}(z - z_1)$$
$$\Rightarrow \theta \equiv G^{-1}[G(z) - \tau] = z_1 + \exp\{\lambda[\lambda^{-1} \log|z - z_1| - \tau]\}\mathrm{sign}(z - z_1)$$

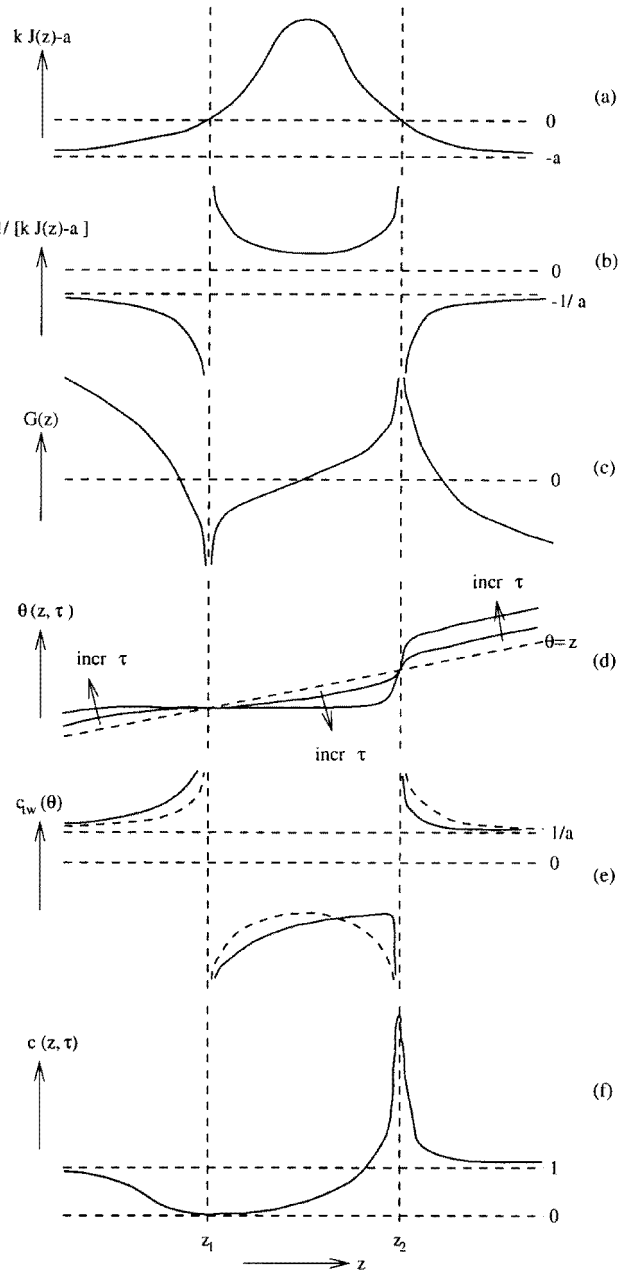

Figure 5. The qualitative form of the various functions involved in the solution of (2) using the method of characteristics. The explanation for these forms is given in the main text. (*a*) illustrates the form of $kJ(z) - a$. We are considering the case $kJ_{\max} > a$, in which case this function has two isolated zeros, at z_1 and z_2, say. (*b*) shows $1/[kJ(z) - a]$, and (*c*) shows its integral, $G(z)$. (*d*) illustrates the form of $\theta(z, \tau)$ as a function of z as τ increases; the broken sloping line is $\theta = z$, which applies when $\tau = 0$. (*e*) shows $c_{tw}(\theta)$ (full curve) compared with $c_{tw}(z)$ (dashed curve); the difference between these curves increases with τ. Finally, (*f*) shows the ratio $c_{tw}(z)/c_{tw}(\theta)$ at one value of τ; this is the solution $c(z, \tau)$ in the case $c_0(x) \equiv 1$.

$$= z_1 + (z - z_1)\mathrm{e}^{-\lambda\tau}$$

$$\Rightarrow c(z,\tau) \equiv c_{tw}(z)/c_{tw}(\theta) = \left[\frac{1}{-\lambda(z-z_1)}\right]\left[\frac{1}{-\lambda(\theta-z_1)}\right]^{-1} = \mathrm{e}^{-\lambda\tau}.$$

Thus the solution for c near $z = z_1$ decreases to zero exponentially in time. Moreover, this calculation is valid whenever both θ and z are close to z_1, so that the region in which c is close to zero remains finite as τ increases.

A similar calculation shows that $c(z_2,\tau) = \mathrm{e}^{+\mu\tau}$, where $\mu = -kJ'(z_2) > 0$, so that c has a maximum at $z = z_2$, whose height increases exponentially with time. However, the width of the peak decreases at a corresponding exponential rate, so that the net amount of connective tissue within this peak ($\propto$ is its area) is roughly constant. This is because the calculation of the solution form near $z = z_2$ is only valid provided $1 \gg |\theta - z_2| = |z - z_2|\mathrm{e}^{\mu\tau}$, that is, provided $|z - z_2| \ll \mathrm{e}^{-\mu\tau}$.

Putting these various calculations together implies that the qualitative form of $c(z,\tau)$ when $kJ_{\max} > a$ and $c_0(x) \equiv 1$ is as illustrated in figure 5(*e*). There is a peak in c at $z = z_1$, whose height and width increase and decrease exponentially in time, respectively, and a trough in c centred at $z = z_1$, whose width increases with time.

For the purposes of illustration, we consider the particular case of nonlinear cellular diffusion, $J_m = m\partial m/\partial x$. In this case, standard analysis [16] shows that the travelling wave solution for cell density that evolves from our initial conditions has the form

$$M(z) = \begin{cases} 1 - \exp\left[\dfrac{z - z_c}{\sqrt{2}}\right] & z < z_c \\ 0 & z > z_c \end{cases}$$

$$\Rightarrow J(z) = \begin{cases} \dfrac{1}{\sqrt{2}}\left(\exp\left[\dfrac{z - z_c}{\sqrt{2}}\right] - \exp[(z - z_c)\sqrt{2}]\right) & z < z_c \\ 0 & z > z_c. \end{cases}$$

Solving the equation $kJ(z) = 1/\sqrt{2}$ shows that

$$z_1, z_2 = \sqrt{2}\log\left(\frac{1 \pm \sqrt{1 - 4/k}}{2}\right).$$

When $k < 4$, these roots are complex, and the travelling wave solution for c exists and is the long-term solution: this solution is

$$c(z) = \begin{cases} \dfrac{\sqrt{2}}{\sqrt{2} - k\sqrt{2}\exp\left(\frac{z - z_c}{\sqrt{2}}\right) + k\sqrt{2}\exp(\sqrt{2}(z - z_c))} & z < z_c \\ 1 & z > z_c \end{cases}$$

for $c_0(x) \equiv 1$. When $k > 4$, however, the solution for c has the aggregating wave form described above; straightforward calculation shows that

$$\lambda = (k/4)\sqrt{1 - 4/k}\left[1 - \sqrt{1 - 4/k}\right]$$

$$\mu = (k/4)\sqrt{1 - 4/k}\left[1 + \sqrt{1 - 4/k}\right].$$

These results are confirmed by numerical simulations of (1); the example of $k = 4.05$ is illustrated in figure 3.

When $c_0(x)$ is not constant, the solution for c is given by multiplying $c_{tw}(z)/c_{tw}(\theta)$ by $c_0(\theta)$. Moreover, this solution is then only exactly valid when $m(x,0)$ is exactly in

travelling wave shape, although since m evolves to the travelling wave shape quite quickly (figures 2(a) and 3(a)), we expect the analysis to determine the key qualitative features of the solution for c. In the case of the step function form of $c_0(.)$, this multiplication by $c_0(\theta)$ has the effect of removing the trough in the solution for $c(z, \tau)$, although the growing peak remains.

5. Predicting lobulation: the case $\theta(c) \neq 1$

In order to study the effects that the accumulation of connective tissue produces on the movement of cells, we choose a suitable function $\theta(c)$ which describes the changes in tumour cell flux owing to the aggregating connective tissue. At low levels, connective tissue does not produce any appreciable effect on the motility of the cells. However, when there is a large amount of accumulated connective tissue this will restrain cell movement. We represent this feature in the form of a decreasing linear ramp function for $\theta(c)$:

$$\theta(c) = \begin{cases} 1 & 0 < c < c_1 \\ \dfrac{c_2 - c}{c_2 - c_1} & c_1 < c < c_2 \\ 0 & c_2 < c. \end{cases} \tag{4}$$

This piecewise-linear form means that for concentrations above the threshold level c_2, cell movement is not possible, while for concentrations below the threshold c_1, there is no impediment to movement arising from connective tissue; this form has no particular mathematical significance other than its simplicity.

When k is sufficiently small, the equations with $\theta(c)$ non-constant have a simple travelling wave solution. This is entirely expected, since if c remains below c_1, there is no inhibition of cell movement. However, as k becomes larger, the solution alters to a new and rather remarkable form, as illustrated in figure 6. The advancing wave of tumour cells is rapidly retarded by the aggregating connective tissue. This aggregating connective tissue wave consequently slows down in parallel, leading to further aggregation, until in the end the waves come to a complete stop. Of course, once the connective tissue concentration has reached the critical value c_2 the area behind this does not show any further change, except due to cell division. However, there is a small residual number of tumour cells ahead of the connective tissue peak at which the waves stop, even though the cell wave is of sharp-front type, and that then restarts the whole process again. This continues until connective tissue once again builds up, and the process is indefinitely repeated, leading to a periodic pattern of tissue. This is analogous to a tumour from which nodules successively bud.

Appealing to the analysis in the previous section, it is easy to see why the tumour cell wave restarts in the form of a nodule. In the solution of (1) with $\theta(c)$ constant, the leading edge of the m wave is at $z = z_c$, while the peak in c occurs at $z = z_2 < z_c$. Thus, there is always a small number of tumour cells ahead of the peak concentration of connective tissue, and we expect this to also be the case for non-constant $\theta(c)$. It is these cells that are responsible for the restarting of the tumour cell wave. However, by comparing the simulation in figure 6 with the case $\theta(c) = 1$, we observe that the progression of the lobulating wave is slower than when unimpeded by connective tissue. This implies that encapsulated tumours grow more slowly as compared with unencapsulated tumours, an observation that agrees well with the biology of tumours [15].

In figure 7 we show the long-term behaviour of the solution. The continued presence of the proliferative ability in the tumour cells, via the source term $f(m)$, causes the cell

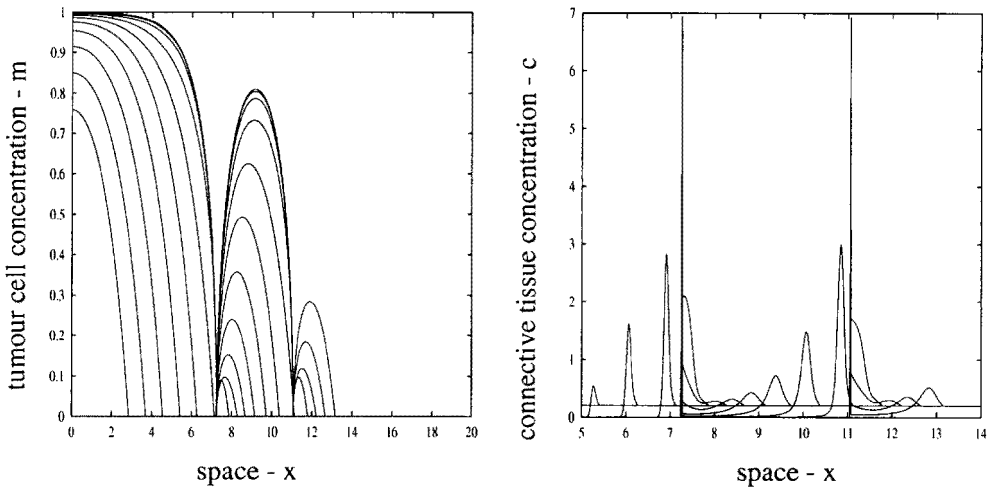

Figure 6. Numerical solutions for (1) with $\theta(c)$ from (4) and $J_m = m\partial m/\partial x$. Initially the wave behaves as in figure 3. However, when the concentration of c crosses the value c_1 the wave slows down as shown by the immediately succeeding plots which are at equal intervals of time measuring 1.2. However, the process starts again. The various curves in the first plot show the contours of different m values. The parameter values used in this simulation are $k = 5$, $c_1 = 3$ and $c_2 = 5$.

density to increase so that adjacent nodules eventually coalesce to form larger ones. Small amounts of connective tissue persist within these nodules. This agrees well with the known morphology of multilobular tumours, as schematically illustrated in figure 1.

A central feature of the solution illustrated in figure 7, and of all solutions of our model, is that the simulated tumour actually continues to grow forever. In practice, of course, tumour growth ceases at a finite tumour size. This cessation of growth has in fact been very well studied and is primarily due to the limited rate at which nutrients can diffuse into a solid tumour [13]. Following this initial diffusion-limited phase of growth, tumours become quiescent until the onset of angiogenesis [11], leading to vascularized (and potentially lethal) growth. The diffusion-limited cessation of avascular tumour growth has been modelled by a number of previous authors over many years [12, 1, 7, 26]. Our philosophy is to exclude this factor, since it is already understood and effectively modelled: consequently our model does not contain a nutrient variable. The resulting simple model has the major advantage of facilitating mathematical analysis.

6. Discussion

The modelling in this paper has demonstrated a novel bifurcation of a travelling wave into a more general wave form, not of constant shape. It also presents a succinct model for the accretion of connective tissue on the surface of a growing tumour.

A new biological mechanism brought to light through this modelling pertains to the formation of tumour nodules. There is currently no satisfactory understanding of why some tumours are multinodular while others are not. The results of this modelling suggest that when the growth of a tumour is unimpeded by any restraining force, it grows without nodularity. However, when accumulating connective tissue significantly inhibits cell motility, the tumour breaks up into nodules. This novel mechanism could be tested

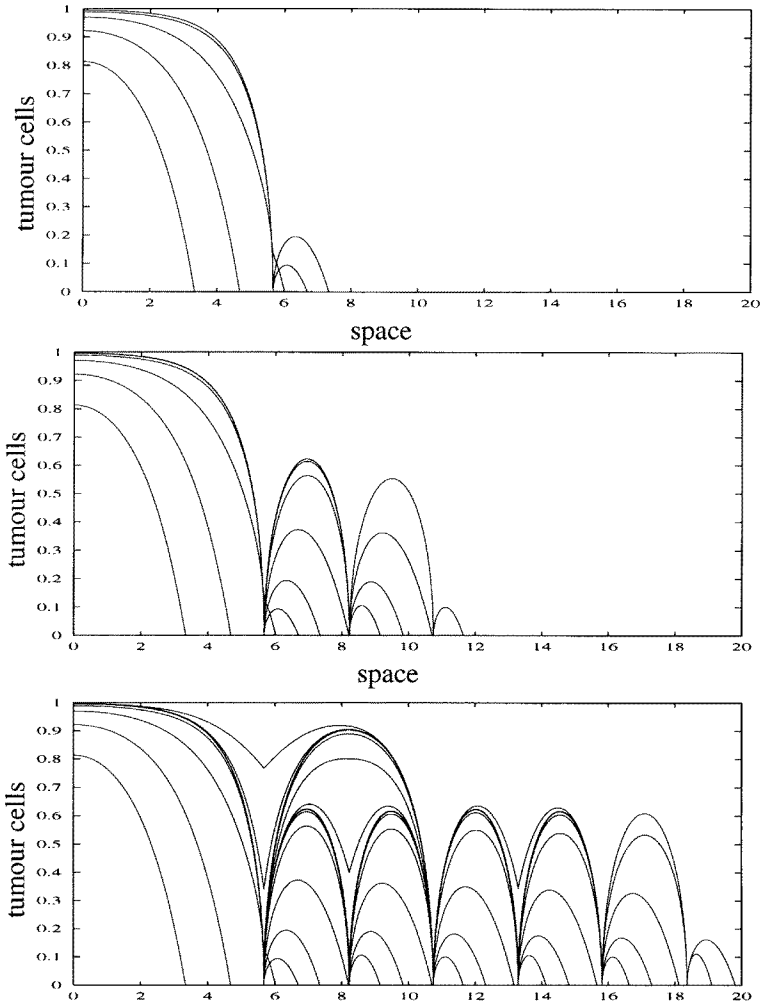

Figure 7. Long-term behaviour of the solutions shown in figure 6 which shows the adjacent nodules growing and coalescing. The various curves in the first plot show the contours of different m values. Since the equation for $m(x, t)$ has a source term $m(1 - m)$, representing cell division, the concentration tends to a value 1. The three frames show the solutions for the tumour cell wave starting from $t = 0$ to $t = 80$, 150 and 250 respectively with each curve plotted at equal intervals measuring 13.9.

in the laboratory by growing tumour nodules in different concentrations of matrix proteins, which are commercially available as matrigel. Thus, the work described in this paper thus provides an example of a potentially testable biological hypothesis arising from theoretical modelling.

The model equations (1) are of course extremely simplistic and neglect a great many features of real tumour growth. A tumour cell interacts with the connective tissue in several ways, depending on the range of mutations it has undergone [2]. Benign tumour cells merely advect and compress surrounding connective tissue, thereby causing encapsulation [8]. Further mutations can make the cells invasive. These mutations can cause the cells to produce large amounts of proteases leading to the digestion of the connective tissue,

or can make the cells sensitive to connective tissue gradients (chemotaxis and haptotaxis) [2] or alter their adhesiveness [19]. These phenotypic changes in a cell allow it to invade neighbouring tissue and to be carried away far from its primary site [23].

When malignant transformation occurs in an encapsulated benign tumour, the capsule is at first disrupted by the action of proteases and the cells can then escape into the surrounding tissue [8]. Clinically, this transcapsular spread represents a crucially important point in the evolution of the tumour. Before transcapsular spread the prognosis for a malignant tumour is favourable, since the tumour can be completely removed by surgery. However, once the capsule has been disrupted, more aggressive forms of surgery (for example, wide dissection) will be required, often in combination with other forms of treatment such as chemotherapy or radiotherapy. More importantly, the final outcome of treatment in patients with transcapsular spread compares poorly with tumours that are confined by the capsule [3].

We conclude this paper by describing the results of simulations of an improved version of the model (1), which incorporates some of the features discussed above. The model includes a study of the behaviour of normal cells which sets the background within which the tumour cells invade. Tumour cells differ from normal cells both in their local behaviour (for example, the loss of contact inhibition and the ability to produce proteases) and in their spatial behaviour (for example, enhanced chemokinesis, chemotaxis and haptotaxis). Here we describe the consequence of a mutation resulting in the loss of contact inhibition and another resulting in the production of a protease by the cancer cells.

When a malignant tumour produces proteases (for example matrix metalloproteases), this typically occurs at the growing edge of the tumour which is in contact with the surrounding connective tissue [27]. The body produces other proteins called antiproteases that have the ability to neutralize the effects of the proteases. Also, as proteases are small biochemicals they can diffuse into the surrounding tissue. This results in the digestion of surrounding connective tissue, providing a mechanism for the possible disruption of the capsule. To study the occurrence of such capsular disruption we expand the model in (1) to incorporate the dynamics of the proteases. The new model has the form

$$\frac{\partial n}{\partial t} = k_1 n(k_2 - n - m) + k_3 \frac{\partial}{\partial x}\left[n \frac{\partial n}{\partial x}\right] \tag{5a}$$

$$\frac{\partial m}{\partial t} = k_4 m(k_5 - n - m) + k_6 \frac{\partial}{\partial x}\left[m \frac{\partial m}{\partial x}\right] \tag{5b}$$

$$\frac{\partial c}{\partial t} = -k_7 pc + k \frac{\partial}{\partial x}\left[cm \frac{\partial m}{\partial x}\right] \tag{5c}$$

$$\frac{\partial p}{\partial t} = k_8 uc - k_9 p - k_{10} up - k_{11} pc + k_{12} \frac{\partial^2 p}{\partial x^2} \tag{5d}$$

where $n(x, t)$ is the concentration of the normal cells and $p(x, t)$ is the concentration of the protease. Here the k_i's are all positive constants. k_1 and k_4 represent the linear growth rates of the normal cells and the tumour cells and k_2 and k_5 represent their maximum carrying capacities. Thus, the difference $k_5 - k_2$ is a measure of the loss of contact inhibition. k_3 and k_6 represent the effective diffusion coefficients of the normal and tumour cells. The interpretation of the various terms in equations (5*c*) and (5*d*) are as follows.

$-k_7 pc$ represents the degradation of connective tissue by the protease

$k_8 uc$ represents the production of the protease at the interface of the tumour and the surrounding tissue

$-k_9 p$ models the natural degradation of the protease

$-k_{10} up$ and $-k_{11} pc$ represent the neutralization of the protease by the action of

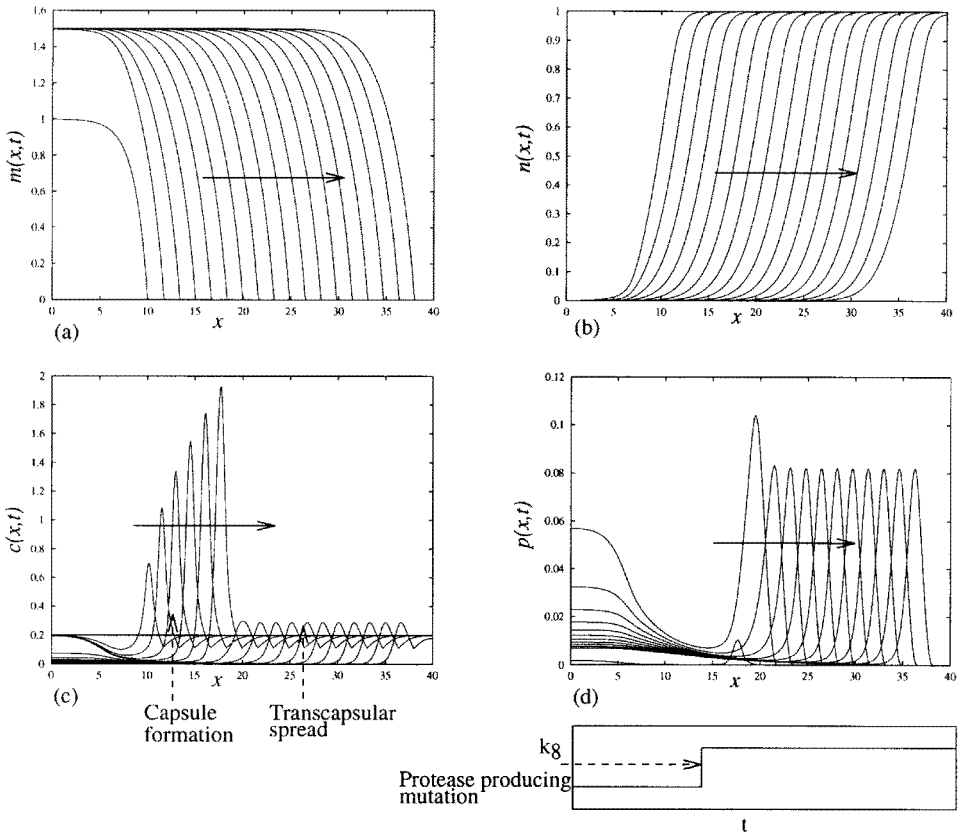

Figure 8. Numerical solution of equation (5) showing the replacement of normal tissue by tumour cells and an incipient capsule being degraded by the action of a protease produced by a mutation in the tumour cell. The occurrence of this mutation is shown in the box below. (*a*) The spatial distribution of the tumour cells with a wave of cells moving to the right. (*b*) The normal cells in a receding wave that is being replaced by the tumour cells. (*c*) The formation of a capsule initially, which is eventually degraded once the mutation has occurred. (*d*) The spatial distribution of the protease. The parameter values used in this simulation are $k_1 = 5$, $k_2 = 1$, $k_3 = 1$, $k = 5$, $k_4 = 1$, $k_5 = 1.5$, $k_6 = 1$, $k_7 = 5$, $k = 5$, $k_9 = 3.1$, $k_{10} = 0.1$, $k_{11} = 0.1$, $k_{12} = 0.1$. The arrows show the direction of increasing time.

antiproteases. The constant k_{12} is the diffusion coefficient of the protease.

In figure 8 we illustrate a typical numerical solution of the improved model (5). In this simulation, we begin solution with $k_8 = 0$, that is, no protease is produced. This results in the formation of a capsule in a manner very reminiscent of the solutions discussed in section 4. Note, however, that in this case there are also the dynamics of the normal cell population to consider; the receding wave of these cells corresponds to their out-competition by the tumour cells. Part-way through the simulation, we alter k_8 to have a positive value, which crudely simulates the occurrence of a mutation resulting in the production of protease by the tumour cells. Once this mutation has occurred and protease production starts, the capsule is disrupted, as shown by the absence of increasing waves of c. In this second part of the solution, the cancer cells can spread unhindered by the capsule.

The simulation illustrated in figure 8 has two key implications. First, it demonstrates capsule formation via the mechanism described earlier in the paper, but in an enlarged and

somewhat more realistic model, adding to the credibility of this mechanism. Secondly, it shows that the mechanism is consistent with postulated methods of capsule disruption. However, it must be stressed that for cancer cells to spread aggressively they need additional mechanisms of motility such as chemotaxis and haptotaxis, and alterations in adhesivity. Work is currently in progress in our group to understand the contribution of these various interactions to cancer invasion.

Appendix: numerical methods

We solved (1) with the functional forms in the three cases using an explicit finite difference scheme. Equations (1) are a mixed hyperbolic-parabolic system of PDEs and appropriate attention must be paid to the differing stability criteria in the two equations. The discretization for (1a) must satisfy the condition $\Delta t_m \leqslant 0.5(\Delta x)^2$, where Δt_m is the parabolic time step and Δx is the spatial step size. The discretization of (1b) must satisfy the CFL condition, that is, $\Delta t_c \leqslant \Delta x/b$ where $b = \theta_c c J + \theta J$, and Δt_c is the hyperbolic time step. We solved the two equations simultaneously using the same step size for the whole system as $\Delta t = \min(\Delta t_m, \Delta t_c)$.

Appropriate upwinding is crucial for the solution of (1b). In solving the case $\theta(c) \neq 1$, note must be taken that appropriate upwinding requires consideration of the sign of $(\theta_c c J + \theta J)$, and not just the coefficient of c_x in (1b).

Acknowledgments

We are grateful to Helen Byrne (UMIST) for helpful discussions. This work was supported in part by a grant from the London Mathematical Society to Philip Maini (Oxford), Mark Chaplain (Bath) and JAS. AJP was funded in part by the a Radhakrishnan Scholarship and in part by a Research Training Fellowship from the Wellcome Trust.

References

[1] Adam J A 1986 A simplified mathematical model of tumour growth *Math. Biosci.* **81** 229–42
[2] Aznavoorian S, Stracke M L, Krutzsch H, Schiffman E and Liotta L A 1990 Signal transduction for chemotaxis and haptotaxis by matrix molecules in tumour cells *J. Cell Biol.* **110** 1427–38
[3] Bailey H *et al* 1995 *Bailey & Love's Short Practice of Surgery* (Chapman and Hall)
[4] Barr L C 1989 The encapsulation of tumours *Clin. Expl. Metastasis* **7** 277–82
[5] Barr L C, Carter R L and David A J S 1988 Encapsulation of tumors as a modified wound healing response *The Lancet* **II** no 8603 135–7
[6] Berenblum I 1970 The nature of tumour growth *General Pathology* ed H E W Florey (London: Lloyd-Luke)
[7] Byrne H M and Chaplain M A J 1995 The growth of non-necrotic tumours in the presence and absence of inhibitors *Math. Biosci.* **130** 151–81
[8] Carter R L *et al* 1985 Transcapsular spread of metastatic squamous cell carcinoma from cervical lymph nodes *Am. J. Surg.* **150** 495–9XC
[9] Enneking W F 1983 *Musculoskeletal Tumour Surgery* (Edinburgh: Churchill Livingstone)
[10] Ewing J 1940 *Neoplastic Diseases* (Philadelphia, PA: Saunders)
[11] Folkman J 1995 Angiogenesis in cancer, vascular, rheumatoid and other disease *Nature Med.* **1** 27–31
[12] Greenspan H P 1972 Models for the growth of a solid tumour by diffusion *Stud. Appl. Math.* **52** 317–40
[13] Groebe K and Mueller-Klieser W 1991 Distribution of oxygen, nutrient and metabolic waste concentrations in muticellular spheroids and their dependence on spheroid parameters *Eur. Biophys. J.* **19** 169–81
[14] Kolmogroff A, Petrovsky I and Piscuonoff N 1937 Étude de l'équation de la diffusion avec croissance de la quantité de matière et son application á un probléme biologique *Moscow Univ. Bull. Math* **1** 1–25
[15] Lai E C S *et al* 1990 Long term results of resection for large hepatocellular carcinomas: a multivariate analysis of clinicopathological features *Hepatology* **11** 815–18

[16] Sanchez-Garduno F and Maini P K 1995 Travelling wave phenomena in some degenerate reaction–diffusion equations *J. Diff. Eqns* **117** 281–319
[17] Murray J D 1990 *Mathematical Biology* (Berlin: Springer)
[18] Ng I O L, Lai E C S, Ng M M T and Fan S T 1992 Tumor encapsulation in hepatocellular carcinoma *Cancer* **70** 45–9
[19] Parsons D F 1993 Tumor cell interaction with stromal elastin and type-i collagen: The consequences of specific adhesion and proteolysis *Tumor Biol.* **14** 137–43
[20] Robbins S L, Cotran R S and Kumar V 1984 *Pathologic Basis of Disease* (Philadelphia, PA: Saunders)
[21] Sherratt J A and Nowak M A 1992 Oncogenes, anti-oncogenes and the immune response to cancer: a mathematical model *Proc. R. Soc.* B **248** 261–71
[22] Sherratt J A and Marchant B P 1996 Non-sharp travelling waves in the Fisher equation with degenerate nonlinear diffusion *Appl. Math. Lett.* **9** 33–8
[23] Stetler-Stevenson W G, Aznavoorian S and Liotta L A 1993 Tumor cell interactions with the extracellular matrix during invasion and metastasis *Ann. Rev. Cell. Biol.* **9** 541–73
[24] Vaidya V G and Alexandro F J Jr 1982 Evaluation of some mathematical models for tumour growth *Int. J Biomed. Comput.* **13** 19
[25] William P L and Gray H 1995 *Gray's Anatomy* (Edinburgh: Churchill Livingstone)
[26] Ward J P and King J R 1997 Mathematical modelling of avascular tumour growth *IMA J. Math. Appl. Med. Biol.* **14** 39–69
[27] Xie B, Bucana C D and Fidler I J 1994 Density-dependent induction of 92-kd type type-IV collagenase activity in cultures of A431 human epidermoid carcinoma cells *Am. J. Pathol.* **144** 1958–67
[28] Zoller M, Goodman M L and Cummings C W 1978 Guidelines for prognosis in head and neck cancers with nodal metastasis *Laryngoscope* **88** 135–40